Adsorption of Triblock Copolymers of Ethylene Oxide and Propylene Oxide at the Air/Water Interface: The Surface Excess

J. B. Vieira, Z. X. Li, and R. K. Thomas*

Physical Chemistry Laboratory, South Parks Road, Oxford, OX1 3QZ, U.K.

Received: August 24, 2001; In Final Form: January 10, 2002

Neutron reflection has been used to measure the surface excesses of two poly(ethylene oxide-*b*-propylene oxide-*b*-ethylene oxide) triblock copolymers (EPE) at the air/water interface over a range of bulk solution concentrations. The copolymers, of approximate formulas $E_{23}P_{52}E_{23}$ and $E_9P_{22}E_9$ and have similiar adsorption isotherms in terms of their molar adsorption, though quite different in terms of segmental adsorption. The isotherms have two steps, one at low concentrations leading to a plateau over about two decades of concentration followed by a substantial rise over the decade of concentration leading to the critical micelle concentration. In the plateau region, the area per ethylene oxide segment was found to be about 9 and 22 Å^2 respectively for the two copolymers decreasing to 6.5 and 12 Å^2 at the CMC at 25 °C. The thickness of the adsorbed layer showed little change between these two coverages. An increase in temperature to 35 °C shifted the adsorption isotherm pattern to concentrations about $^1/_{30}$ of those at 25 °C, in line with the change in CMC. The neutron surface excesses were incorporated into the integrated Gibbs equation and fitted the surface tension curves well over most of the range of adsorption. However, a sharp change in surface tension at low polymer concentrations (about 10^{-3} wt/vol %) was found not to be consistent with the neutron measurements, and a model of the surface tension behavior in this region, based on adsorption from a polydisperse sample, has been proposed to explain this behavior. Earlier explanations of this surface tension behavior are shown to be inconsistent with the neutron reflection and surface tension results.

Introduction

Triblock copolymers between ethylene oxide and propylene oxide (EPE) are very effective surfactants and are commercially available under the tradenames Pluronic or Synperonic. Their effectiveness as surfactants is evident from their widespread usage in a range of industrial applications, including detergency, dispersion, stabilization, foaming, and emulsification.[1−4] One of their main advantages is that their strong adsorption at oil/water and air/water interfaces provides an effective steric barrier that prevents flocculation and/or coalescence of emulsion droplets and foam bubbles. The adsorption characteristics of EPE triblock copolymers are therefore fundamental to an understanding of the role of these copolymers in such applications.

The surface tension profile of EPE copolymers at the air/water interface has been found to be more complicated than for small molecule surfactants. Two inflections (breaks) are found in the surface tension vs log concentration ($\gamma - \log c$) curve for most commercial triblock samples, and depending on which part of the curve is taken to be consistent with the Gibbs isotherm, quite different values are obtained for the area per adsorbed molecule or surface excess. For example, Prasad et al. made measurements over a broad concentration range on seven Pluronics at 20 °C and in all cases observed the existence of the two breaks, but no clear plateau region of the surface tension even up to concentrations of 10 wt/vol %.[5] They attributed the low concentration break that generally occurs in the vicinity of 10^{-3} wt/vol % to the formation of monomolecular micelles, suggesting that a conformational change of the single copolymer chain may lead to a close-packed entity with the hydrophobic block coiled in the interior and shielded by the hydrophilic EO segments. Wanka et al.[6] attributed the two breaks in the $\gamma - \ln c$ plot for Pluronic P127 to the broad molecular distribution of the copolymer, suggesting that the most surface-active fraction starts to associate in solution at the first break point (10^{-3} wt/vol %) and that the less surface-active material, which makes up the bulk of the sample, forms micelles at the second break point. Alexandridis et al.[7] used the results from materials having the same size of PO block but different EO block lengths, as well as Pluronic surfactants with the same EO/PO ratio but different total molecular weight, to argue that neither polydispersity nor impurities could be responsible for the low concentration break point. They again suggested that the origin of this break arises from the rearrangement of the Pluronic molecules to a more compact structure in the adsorbed layer. Linse & Hatton,[8] using a mean field calculation, concluded that the origin of the low concentration break lies in the depletion of the bulk phase by adsorption at the surface. Thus, when the molar concentration of polymer is sufficiently low, adsorption at the surface depletes the bulk solution to such an extent that the surface tension behavior comes to be dominated by the depletion.

It is relatively straightforward to establish the presence of micelles in the bulk solution, and the upper concentration break point has been definitively assigned to the CMC. However, to establish what is happening at the surface below this concentration requires a method that can determine surface structure and composition and such a method is neutron reflection.[9] There are two difficulties in carrying out neutron reflection studies; one is that it is necessary to have deuterated polymer, and the other, which is evident from the above discussion, is that

* To whom correspondence should be addressed. Phone: 0044-1865-275422. Fax: 0044-1865-275410. E-mail: thomas@ermine.ox.ac.uk.

10.1021/jp013286i CCC: $22.00
Published on Web 05/03/2002

TABLE 1: Molecular Characteristics of the EPE Copolymers

formula	M_n	%EO	M_w/M_n
$E_{23}P_{52}E_{23}$	4900	41	1.03
$dE_{23}P_{52}dE_{23}$	5000	42	1.03
$E_9P_{22}E_9$	2000	40	1.04
$dE_9P_{22}dE_9$	2000	42	1.03

impurities and polydispersity may play a role in determining the surface behavior. We have therefore synthesized our own deuterated materials to a higher level of purity and monodispersity than typically characteristic of commercial samples. In this paper, we compare measurements of surface tension with direct measurements of surface excess using neutron reflection. As we have shown previously, the reconciliation of neutron surface excesses with surface tension data is a powerful way to assess the surface behavior.

Experimental Details

Preparation and Characterization of EPE Copolymers. For each composition and molecular weight of copolymer, two isotopic species were synthesized, fully protonated poly(ethylene oxide-*b*-propylene oxide-*b*-ethylene oxide), designated EPE and a matching sample of dEPdE where the d denotes that the ethylene oxide was deuterated. The polymer was prepared by reacting commercially available polypropylene glycols (Aldrich) with ethylene oxide using a synthetic route similar to that of Altinok et al.[10] The polypropylene glycol was first dried under a vacuum at 60 °C for 24 h. Potassium *tert*-butoxide (Aldrich) (1 M in dry tetrahydrofuran) was added in an amount sufficient to convert about 60% of the OH groups to OK. Following stirring, *tert*-butyl alcohol and THF were removed under vacuum, again warming to about 60 °C. Dry, freshly distilled THF was added to the mixture, and an accurately measured quantity of ethylene oxide in a sidearm was allowed to react through the vapor phase with the stirred solution, with all air having previously been removed. The solution was initially held at 30 °C for about 24 h and then heated at 40 °C. The reaction was generally complete within the first 24 h but was usually left for 2−5 days at the higher temperature. The ethylene oxide in the sidearm of the reaction vessel was distilled from CaH_2 and was held at room temperature or below to prevent any build-up of excessive pressure. The reaction was terminated by adding hydrochloric acid, and solvent and water were then removed under vacuum. The product was dissolved in dichloromethane and dried with magnesium sulfate, and NaCl and $MgSO_4$ were removed by filtration. The product was then thoroughly washed with hexane to remove any residual polypropylene glycol. The deuterated ethylene oxide chain dEPdE copolymer was prepared following the same procedure but with deuterated ethylene oxide, kindly supplied by Dr. D. A. Styrkas.

The starting polypropylene glycol and the EPE copolymers were characterized by gel permeation chromatography (GPC) (30 cm Mixed-E column (Polymer Laboratories), THF elutant, flow rate 1 mL min^{-1}). The calibration used a series of PEO standards (Polymer Laboratories). The GPC results are listed in Table 1. We found that the polypropylene glycol starting materials were sufficiently monodisperse for nominal molecular weights of 3000 and below that we could prepare final copolymer molecular weights with a precision of about 10 wt %, and these final samples showed a reasonable monodispersity. The GPC patterns of our materials showed that our samples were of much higher purity and monodispersity than the nearest comparable commercially available Pluronic. An interesting observation was that our samples dissolved in water in a few minutes, whereas the commercially available sample nearest in composition and molecular weight required the best part of 24 h to dissolve. We attribute this to the presence of a significant fraction of residual PPO in the commercial Pluronic. Because this is highly hydrophobic it is of particular importance for the surface tension behavior. A list of the materials prepared and studied is given in Table 1.

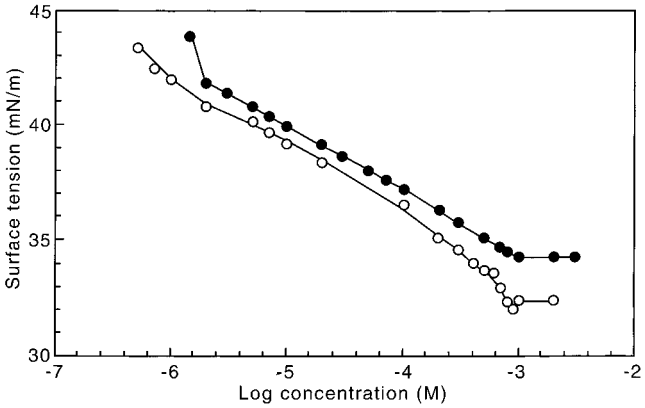

Figure 1. Surface tension−log concentration curves for solutions of Pluronic P105 (o) and $E_{23}P_{52}E_{23}$ copolymer (•) measured at 25 °C using the du Noüy ring.

Surface tension measurements were carried out using a Kruss K10 maximum pull tensiometer fitted with a 19.1 mm diameter Pt/Ir ring. The usual precautions were taken to ensure cleanliness. Stock solutions of the block copolymers were prepared using ultrapure water and were diluted down to obtain the desired concentration. Temperature control within 0.5 °C was maintained using water circulated from a refrigerated water bath. The platinum ring was flamed until red-hot and washed copiously with pure water before each measurement. All measurements were repeated until a consistent reading was attained. The surface tension readings were subsequently corrected using correction factors compiled by Harkins and Jordan.[11]

The neutron reflection measurements were made on the white beam reflectometer SURF based at the ISIS pulsed neutron source at Rutherford-Appleton Laboratory, Didcot, U.K.[12] The detailed experimental procedure for performing the measurements with a single detector has been described previously. The measurements were made at fixed incident angles of 0.8° and 1.5°. The reflectivities obtained at both angles were subsequently combined into a single reflectivity profile and calibrated with respect to D_2O. Flat backgrounds measured at high momentum transfer were subtracted for all measurements prior to data analysis. The solutions of copolymers were poured into Teflon troughs mounted on an antivibration bench. High purity water was used for all of the measurements, and all of the glassware and the Teflon troughs were cleaned using alkaline detergent (Decon 90) followed by rinsing with ultrapure water.

Results and Discussion

Surface Tension. The variation of the surface tension γ of aqueous solutions of $E_{23}P_{52}E_{23}$ with log(concentration), measured at 25 °C using the du Noüy ring, is shown in Figure 1. Two breaks, one at low concentration and one at high concentration, are observed in the γ − log c curve. The high concentration breakpoint occurs at a concentration of 9.5×10^{-4} M. Above this concentration, the surface tension remains unchanged with increasing polymer concentration, and this

concentration is therefore assumed to be the CMC. Between the CMC and the low concentration break, a second-order polynomial could be fitted to the increase of surface tension with decreasing bulk concentration. It has the convex curvature expected from the Gibbs equation for an increase in copolymer adsorption with bulk concentration. The low concentration break occurs at 2×10^{-6} M. Below this break was a region where the surface tension readings were inconsistent and could not be reliably assessed. When compared with Pluronic P105, which is the nearest commercially available equivalent (Figure 1), the $\gamma - \log c$ curve for $E_{23}P_{52}E_{23}$ has similar features in that both curves show the two breaks.

The CMC for P105 is reached at 8.0×10^{-4} M which compares with values of 3.5×10^{-4} and 8.0×10^{-4} M obtained by the dye solubilization method.[13,14] Pluronic P105 is a polydisperse material, and some variation in CMC is to be expected between different samples. For our sample of P105, a minimum in the vicinity of the CMC also occurred in the surface tension curve, which can be attributed to the replacement of highly surface active impurities at the interface by the major and less surface-active component as the surface active impurities are solubilized in the micelles formed by the major component. The curvature of the region between the CMC and the low concentration break was more pronounced in P105 than for $E_{23}P_{52}E_{23}$. The low concentration break for P105 was attained at a copolymer concentration of 10^{-6} M, but in this region, there were large differences between our surface tension curve and those already published, in which the Wilhemy plate method was used.[7,15] We therefore remeasured the surface tensions of both P105 and $E_{23}P_{52}E_{23}$ using the Wilhelmy plate, which led to a satisfactory agreement with the previously published work for P105. It was evident that the surface tension of Pluronic P105 solutions could be measured with the plate down to 1.5×10^{-8} M but only down to 5.0×10^{-7} M with the ring. Below these concentrations, just as found for $E_{23}P_{52}E_{23}$, the results obtained were always inconsistent and unreliable. When using the Wilhemy plate on $E_{23}P_{52}E_{23}$, the low concentration break point was found at a lower concentration, approximately 5×10^{-7} M, and below this concentration, there was a steep increase in the slope of the curve (the two plots are compared in Figure 9, although in somewhat modified form). We attribute the lack of consistency with the du Noüy method at low copolymer concentration to the inability of the EPE copolymers to diffuse to the surface on the time scale of the measurement, which is shorter for the ring than for the plate. Reports of such factors being important have been made by others.[16,17] The sensitivity of the low concentration break to the measuring technique suggests that the nature of this break may be associated with nonequilibration, and this will be discussed further below. Although the two techniques perform differently at concentrations in the vicinity of the low concentration break point, they agree well at concentrations above 10^{-5} M.

One of the other copolymers of the same composition but a much lower molecular weight was studied, and the results for this ($E_9P_{22}E_9$) are compared with $E_{23}P_{52}E_{23}$ in Figure 2. The values for the CMCs, the maximum surface pressure, Π_{max}, the surface concentration of the saturated monolayer, Γ_{sat}, and the area per copolymer molecule, A, are summarized for the various EPE copolymers in Table 2. The data show that the surface activity of EPE copolymers is very sensitive to the copolymer molecular weight, as has been found for the commercial versions of these polymers (see, for example, ref 4).

The surface tensions of the EPE copolymer solutions were also measured at 35 °C, and the surface tension curves obtained

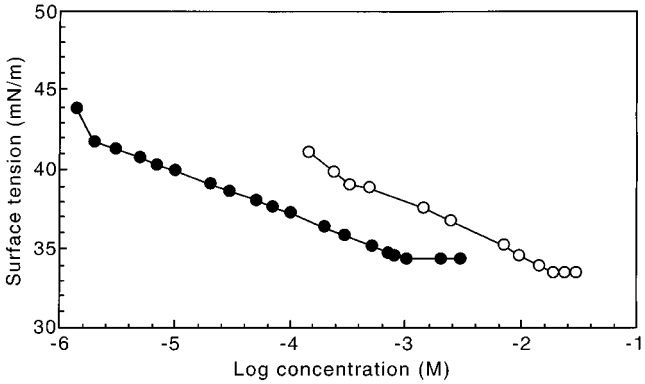

Figure 2. Surface tension−log concentration curves for solutions of EPE copolymers at 25 °C for $E_9P_{22}E_9$ (o) and $E_{23}P_{52}E_{23}$ copolymers (•).

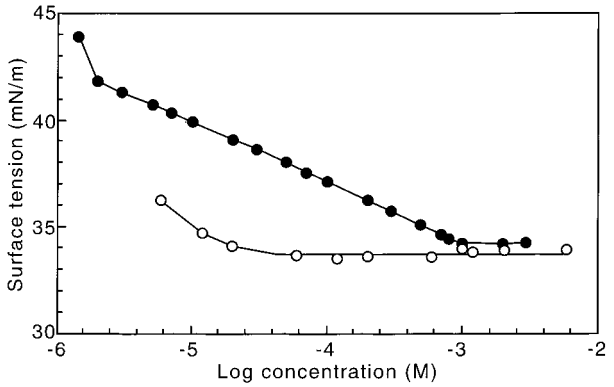

Figure 3. Effect of temperature on the surface tension: $\gamma - \log c$ plots for $E_{23}P_{52}E_{23}$ copolymer measured at 25 (•) and 35 °C (o).

TABLE 2: Surface Characteristics of the EPE Copolymers Determined from Surface Tension Measurements

copolymer	CMC/ M	$\Pi_{max} \pm 0.2$/ mN m^{-1}	Γ_{sat}/ mol m^{-2}	$A_{seg} \pm 0.5$/ Å^2
$E_{23}P_{52}E_{23}$ (25 °C)	9.5×10^{-4}	37.7	5.4×10^{-7}	6.7
$E_{23}P_{52}E_{23}$ (35 °C)	2.7×10^{-5}	38.0	7.3×10^{-7}	5.0
$E_9P_{22}E_9$ (25 °C)	1.8×10^{-2}	38.6	7.5×10^{-7}	12.3
$E_9P_{22}E_9$ (35 °C)	6.1×10^{-4}	39.3	1.2×10^{-6}	7.8
Pluronic P105	5.9×10^{-4}	39.6	8.0×10^{-7}	4.6

at 25 and 35 °C for the $E_{23}P_{52}E_{23}$ copolymer are shown in Figure 3. The surface activity of the EPE copolymers is markedly increased by an increase in temperature, as had also been found previously for commercial EPE copolymers. The CMC values decrease by more than 1 order of magnitude on increasing the temperature from 25 to 35 °C. In the strong temperature dependence of their surface activity, EPE copolymers differ greatly from C_nE_m surfactants, whose CMCs are much less affected by temperature. Thus, the CMC for $C_{12}E_8$ at 15 °C is 9.7×10^{-5} M, and at 40 °C, it only drops down to 5.8×10^{-5} M. As the micellization of EPE copolymers is mostly dictated by the PO block, an increase in temperature should lead to an increase in the surface activity and a lower CMC because of the strongly enhanced hydrophobicity of the PO block. The mechanism behind the temperature dependence of the hydrophobicity of the PO blocks is still not agreed. Malmsten et al. have studied the effect of temperature on the conformation of the −OCCO− segment and shown that the increase of temperature induces a reversible conformational change in the −OCCO− fragment of the PO group, which therefore assumes a less polar conformation.[18] The solvation of this less polar PO group by water is consequently impaired, rendering the solute−solvent interaction less favorable and hence making the PO more

TABLE 3: Scattering Properties of the Components of the Layer

species	scattering length/Å	molecular vol/Å^3	scattering length density/Å^{-2}
dEO	4.40×10^{-4} (96%D)	64.6	6.81×10^{-6}
hEO	4.14×10^{-5}	64.6	0.64×10^{-6}
hPO	3.31×10^{-5}	96.5	0.34×10^{-6}
D_2O	1.91×10^{-4}	30	6.35×10^{-6}
H_2O	-1.68×10^{-5}	30	-0.56×10^{-6}
NRW	0	30	0

hydrophobic. The CMC, maximum surface pressure, Π_{max}, saturated surface concentration, Γ_{sat}, and area per molecule, A, at 35 °C are given in Table 2.

The surface tensions at the CMC are higher than the small molecule C_nE_m surfactants where values as low as 25 mN m^{-1} are found.[19] However, although the surface tension of the EPE copolymers is higher than their small molecule counterparts at the CMC, this is reversed at lower concentrations. As the concentration decreases, the EPE copolymers become relatively more and more efficient in reducing the surface tension. This is mainly a consequence of the Gibbs equation combined with the large molar surface area of the polymers in comparison with the much smaller molar area of the C_nE_m. Thus, the surface tension of solutions of EPE copolymers studied here increases by only 5−10 mN m^{-1} when the bulk copolymer concentration drops by 2 orders of magnitude below the respective copolymer CMC. For the series of C_nE_8 ($n = 9-14$) surfactants, the surface tension of their solutions increases by 20−30 mN m^{-1} on reducing the bulk concentration by the same range below the CMC.[20]

A clear difference between the surface tension curves presented here and those of commercial Pluronic surfactants relates to the low-concentration break. Alexandridis et al. observed that the concentration at this break was independent of molecular weight. However, Figure 2 shows that is not the case for our two EPE copolymers. The concentration at the first break increases on decreasing the molecular weight of the copolymer. Below the low concentration break, there is always a region of instability and lack of reproducibility (with the ring). This behavior is probably related to the effect of the low diffusion rate of EPE copolymers on the stability of the meniscus formed by the ring. Glass[17] studied the adsorption of poly(ethylene oxide)s at the aqueous−air interface and observed a decrease in rate of adsorption with decreasing bulk concentration and decreasing molecular weight. He suggested that the lower diffusion rate at lower molecular weights was a result of a diminishing entropic contribution to adsorption, i.e., a reduction in the driving force for adsorption. Whether such a suggestion is correct and whether it extends to the triblock EPE copolymers, we cannot judge. We will propose below, on the basis of a comparison between surface tension and neutron measurements, an alternative explanation of the low concentration break. In this explanation, the apparently anomalous behavior of the smaller molecular weights is that their behavior is less affected by polydispersity than that of the higher molecular weight samples, but we defer this discussion until we have examined the neutron results.

Neutron Reflectivity. For a solution of deuterated EO chain $dE_{23}P_{52}dE_{23}$ in null reflecting water (NRW), no neutrons are reflected from the water, and the reflected signal is only from dEPdE copolymer adsorbed at the surface. Furthermore, as can be seen from Table 3, the scattering length density of the PO part of the copolymer is also negligible, and hence, the reflected signal to a good approximation arises entirely from the deuterated EO fragments. Thus, the experiment gives directly the surface excess of EO segments at the interface. The reflectivity profiles at various $dE_{23}P_{52}dE_{23}$ concentrations at 25 °C are shown in Figure 4. The reflectivity normally decreases rapidly with increasing scattering vector (κ), but the profiles in Figure 4 decrease more rapidly than they would for a small molecule surfactant, indicating that the layer is significantly thicker than a small molecule surfactant layer. The reflectivity curves were fitted to a model of the EO segments as a single uniform layer, and the best fits of this model to the data are shown as continuous lines in Figure 4, and the parameters of the fits are given in Table 4. Although a single uniform layer is not a realistic model, the calculated amount of an adsorbed species is usually found to be approximately independent of the shape of its distribution. On the other hand the thickness of the layer, also derived from the fitting procedure, can only be regarded as an approximate value in the absence of more detailed study.

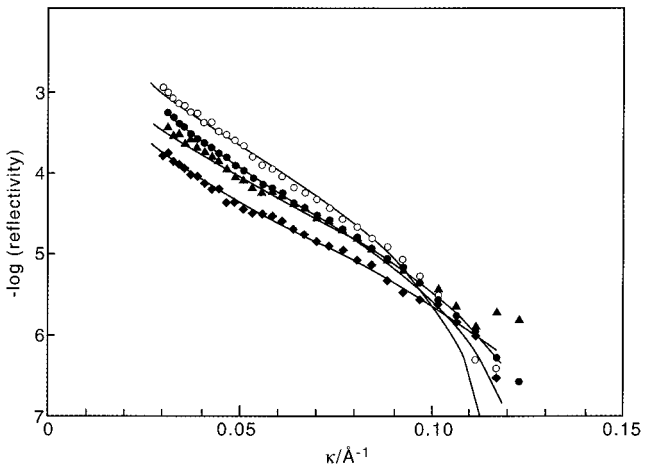

Figure 4. Neutron reflectivity profiles for $dE_{23}P_{52}dE_{23}$ in null reflecting water at 25 °C: 1.2×10^{-3} (o), 1.0×10^{-4} (•), 2.0×10^{-6} (▲), and 2.0×10^{-8} M (◆). The fitted lines are the best fits for a single uniform layer model using the parameters in Table 4.

TABLE 4: Parameters of $dE_{23}P_{52}dE_{23}$ Determined from Neutron Reflectivity Profiles at 25 °C[a]

conc/ M	τ/ Å	$\rho \times 10^6$/ Å^{-2}	A_{seg}/ Å^2	A_{mol}/ Å^2	$\Gamma \times 10^7$/ mol m^{-2}
1.2×10^{-3}	54±2	1.37	6.4	297	5.6 ± 0.3
6.0×10^{-4}	54	1.30	6.8	313	5.3
2.0×10^{-4}	53	1.15	7.8	360	4.6
1.0×10^{-4}	50	1.07	8.9	410	4.0
6.0×10^{-5}	49	1.09	8.9	411	4.0
2.0×10^{-5}	47	1.08	9.4	432	3.8
2.0×10^{-6}	47	1.01	10.0	462	3.6
1.0×10^{-6}	47	0.88	11.5	530	3.1
2.0×10^{-7}	43	0.81	13.7	630	2.6
2.0×10^{-8}	44	0.70	15.5	712	2.3

[a] The values of A_{seg} refer to the area per ethylene oxide segment.

The surface excesses of $dE_{23}P_{52}dE_{23}$ obtained from the neutron reflectivity profiles are plotted as a function of concentration in Figure 5, and this plot can be divided into four regions. In the section labeled D, below 5×10^{-6} M, the surface excess increases gradually with increasing bulk concentration. In section C, which lies between 5×10^{-6} and 10^{-4} M, the surface excess remains almost unchanged with concentration. There is then a steep increase of surface excess with concentration above 10^{-4} M (section B). Although the surface excess increases by almost 40% between 10^{-4} and 1.2×10^{-3} M, the thickness of the monolayer does not change significantly over

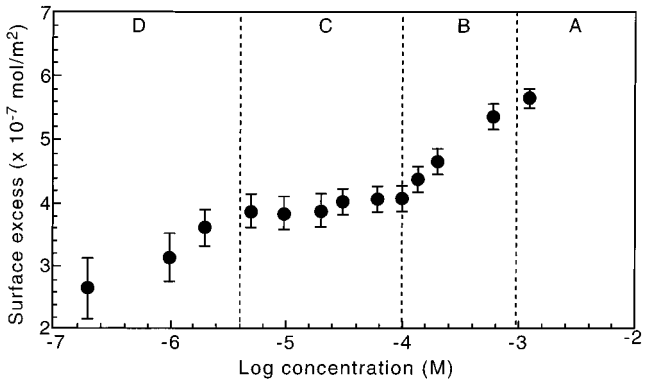

Figure 5. Adsorption isotherm of $dE_{23}P_{52}dE_{23}$ at the air−solution interface at 25 °C determined by neutron reflection.

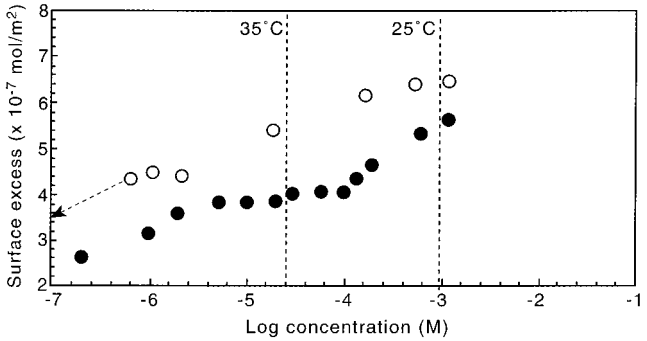

Figure 6. Adsorption isotherms of $dE_{23}P_{52}dE_{23}$ at 25 (•) and 35 °C (o) at the air−solution interface determined by neutron reflection. The vertical dashed lines mark the positions of the critical micelle concentrations of the copolymer at the two temperatures.

TABLE 5: Parameters of $dE_{23}P_{52}dE_{23}$ Determined from Neutron Reflectivity Profiles at 35 °C[a]

conc/ M	τ/ Å	$\rho \times 10^6$/ Å^{-2}	A_{seg}/ Å^2	A_{mol}/ Å^2	$\Gamma \times 10^7$/ mol m^{-2}
1.2×10^{-3}	54 ± 2	1.52	5.8	267	6.2 ± 0.3
2.0×10^{-4}	54	1.51	5.8	269	6.2
2.0×10^{-5}	52	1.40	6.5	301	5.5
2.0×10^{-6}	45	1.27	8.3	384	4.3
2.0×10^{-8}	45	0.89	11.9	548	3.0

[a] The values of A_{seg} refer to the area per ethylene oxide segment.

this range, implying that the increase in surface excess in section B results neither from bilayer formation nor from surface micellization. Note that region B is still below the CMC. An increase in surface excess with no change of thickness must be associated with a significant structural change within the monolayer. Section A is where the bulk solution is micellar and, although not many data have been collected above this concentration, there appears to be a much more gradual increase in the surface excess with bulk concentration in this section.

The reflectivity of $dE_{23}P_{52}dE_{23}$ solutions in NRW was also measured at 35 °C. Using the same methods of analyzing the data as for the lower temperature gives the results of Table 5 and the adsorption isotherm shown in Figure 6. The surface tension measurements have already indicated that the CMC is greatly lowered from 9.5×10^{-4} M at 25 °C to 2.7×10^{-5} M at 35 °C. The neutron results at the higher temperature show that the surface becomes saturated above the CMC and that in the region above the CMC the surface coverage is little affected by temperature. From the slope of the reflectivity profiles, it also appears that temperature has little effect on the thickness of the layer.

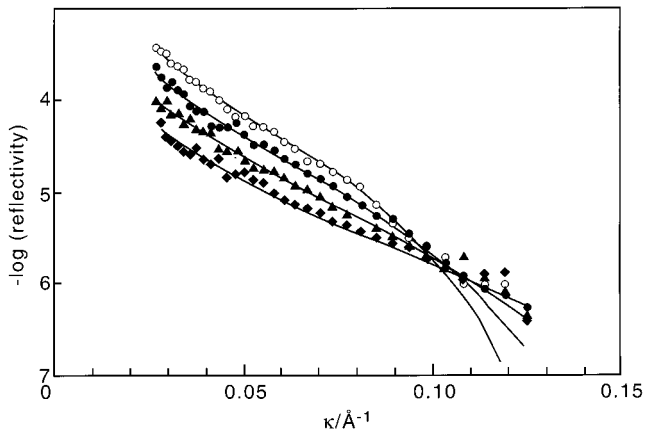

Figure 7. Neutron reflectivity profiles for $E_9P_{22}E_9$ in null reflecting water at 25 °C: 2.8×10^{-3} (o), 1.4×10^{-4} (•), 2.3×10^{-5} (▲), and 1.4×10^{-7} M (◆). The fitted lines are the best fits for a single uniform layer model using the parameters in Table 6.

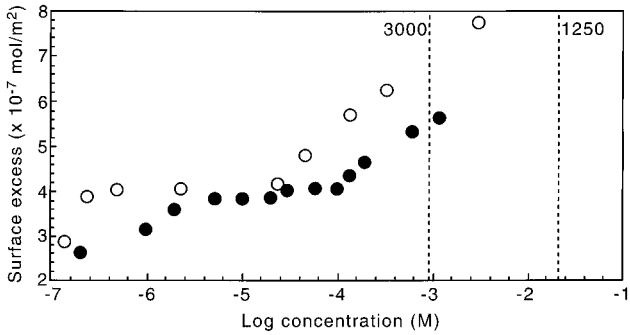

Figure 8. Adsorption isotherms of $dE_{23}P_{52}dE_{23}$ (•) and $E_9P_{22}E_9$ (o) at the air−solution interface at 25 °C determined by neutron reflection. The vertical dashed lines mark the positions of the critical micelle concentrations of the two copolymers.

TABLE 6: Parameters of $dE_9P_{22}dE_9$ Determined from Neutron Reflectivity Profiles at 25 °C[a]

conc/ M	τ/ Å	$\rho \times 10^6$/ Å^{-2}	A_{seg}/ Å^2	A_{mol}/ Å^2	$\Gamma \times 10^7$/ mol m^{-2}
2.8×10^{-3}	49 ± 2	0.82	11.9	215	7.7 ± 0.3
4.7×10^{-4}	45	0.77	13.8	249	6.7
3.3×10^{-4}	44	0.73	14.9	269	6.2
1.4×10^{-4}	44	0.67	16.3	293	5.7
4.7×10^{-5}	41	0.60	19.5	351	4.7
2.3×10^{-5}	39	0.55	22.3	402	4.1
2.3×10^{-6}	36	0.59	22.6	406	4.2
4.7×10^{-7}	36	0.58	22.9	413	4.0
2.3×10^{-7}	33	0.61	23.8	429	3.9
1.4×10^{-7}	32	0.47	31.9	574	2.9

[a] The values of A_{seg} refer to the area per ethylene oxide segment.

The reflectivities of solutions of the much lower molecular weight $dE_9P_{22}dE_9$ were measured at 25 °C, and the reflectivity profiles are shown in Figure 7, where the continuous lines are reflectivities calculated for the uniform single layer model, for which the fitted parameters are given in Table 6. The surface excesses of $dE_{23}P_{52}dE_{23}$ and $dE_9P_{22}dE_9$ are compared in Figure 8 and, interestingly, show similar adsorption patterns in terms of molar adsorption, although in terms of the mass of material adsorbed per unit area the two polymers are completely different. Note that the low molecular weight polymer often has the higher *molar* coverage, but the number of segments (or the mass of material) is nevertheless always lower. The distinct sections observed in the adsorption isotherm of $dE_{23}P_{52}dE_{23}$ are also evident for $dE_9P_{22}dE_9$.

Discussion

For a surface at equilibrium, neutron reflection and the application of the Gibbs equation to the $\gamma - \log c$ plot should give identical surface excesses, and this has always been found to be the case for nonionic surfactants.[9] However, it is not easy to apply the Gibbs equation to polydisperse systems because, in principle, it should be applied separately to each component. In a multicomponent system, even with the simplification that the concentration of each componment is related to the overall concentration, such a treatment would require not only a knowledge of the concentration of all of the constituent species but would also require assumptions to be made about the thermodynamics of surface mixing. These difficulties have been discussed in the outline by Fleer et al.,[21] although in the absence of data that could define the surface accurately.

As can be seen from Tables 2, 4, 5, and 6, there is reasonably good agreement between the results from neutron reflection and those from the Gibbs isotherm in sections B and C of the adsorption isotherm, but there are inconsistencies in region D, i.e., the concentration range just below the low concentration break (see Figure 8). The best method of comparison of the two methods, as has been shown previously, is to use the surface excesses determined from neutron reflection in combination with a single measurement of the surface tension to predict a surface tension curve for comparison with the actual surface tension data.[22] This has the advantage that only a single measurement of the surface tension is used, usually at the CMC, where the measurement is also usually completely reliable, and it avoids the large inaccuracies in determining the slope of the tangent to the $\gamma - \log c$ plot. Thus, the Gibbs isotherm for a neutral species is

$$-\frac{1}{RT}\frac{\mathrm{d}\gamma}{\mathrm{d}\ln a} = \Gamma \qquad (1)$$

where γ is the surface tension, a is the activity, and Γ is the relative surface excess. On integration we obtain

$$\gamma - \gamma_0 = -RT\int_{c_0}^{c}\Gamma(c)\,\mathrm{d}\ln c \qquad (2)$$

where γ_0 is the reference surface tension at the chosen concentration c_0. To facilitate the integration of eq 2, it is better to use a functional form for the neutron excess. We found that the neutron surface excess below the CMC could be well fitted by a quadratic equation in ln c, and this was used for the integration. As pointed out by Linse and Hatton,[8] it is also necessary to take into account surface depletion of the bulk solution. Taking the known volume of the troughs used for the neutron measurements (about 50 cm^3) and the measured neutron surface excesses gave the result that surface depletion only becomes really significant as the nominal bulk concentration decreases toward 10^{-7} M. Because we had measured neutron excesses down to nominal bulk concentrations of 2.0×10^{-8} M, we were able to calculate the surface tension down to concentrations well into the depletion region. The results are shown in Figure 9.

The failings of the ring in comparison with the Wilhelmy plate are evident in Figure 9 as already described. However, it is also evident that the Wilhelmy plate and neutron data disagree, even after allowing for surface depletion effects. In fact, the disagreement starts at concentrations that are too high for there to be significant depletion effects. We believe that a plausible explanation of the discrepancy is one that has been suggested by An et al.[23] for water soluble homopolymers and which we now describe.

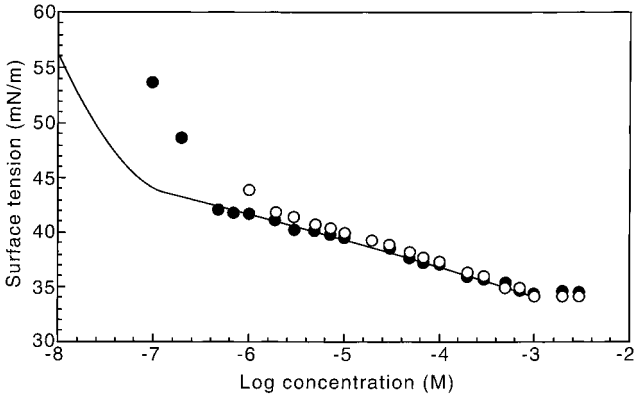

Figure 9. Surface tension as a function of log concentration for $E_{23}P_{52}E_{23}$ at 25 °C measured by the du Nouy ring (o), the Wilhelmy plate (•), and calculated from the neutron surface excesses for $dE_{23}P_{52}$-dE_{23} (continuous line). The effects of surface depletion have been included in the calculation of the bulk concentrations for the neutron curve.

For the purposes of illustrating how polydispersity might contribute to the surface tension upturn, we make two simplifying assumptions about the polymer. These are (i) when the surface is saturated the surface activity of a polymer segment is independent of the molecular weight of the polymer and (ii) the segmental surface coverage remains constant over a large range of bulk concentrations below that required to saturate the surface. Both assumptions are in approximate agreement with experimental obervations on water soluble polymers at the air/water surface. The result of these two assumptions is that equilibrium $\gamma - \ln c$ curves for a series of different molecular weights of a homopolymer follow the straight lines shown in Figure 10, where the upper concentration is the limiting value at which the surface tension is the same for all species. The different slopes of the lines simply reflect the change in molar surface excess in circumstances where the segmental surface excess is independent of molecular weight. The real curves would follow the dashed lines because the surface excess, and hence the magnitude of the slope, must decrease as the concentration decreases. In terms of the bulk *molar* concentration, the surface activity increases with molecular weight. For a homopolymer of finite dispersity, the higher molecular weights of the mixture therefore tend to occupy the surface preferentially and this fractionation is even more pronounced at lower concentrations. If all species were in equilibrium with the surface, the lower molecular weight species would be preferentially displaced from the surface as the concentration was lowered. The surface tension would therefore tend to follow the pattern for the high molecular weight fractions (lowest curve in Figure 10) and remain low as the concentration was lowered. This could not happen indefinitely because it would be limited either by depletion of the high molecular weights from the bulk solution or because the slower diffusion of the high molecular weight species would mean that they were replaced by the more rapidly diffusing lower molecular weight species. In either case, the surface tension curve has to change over from the relatively gradual curve characteristic of high molecular weights to the steeper curves characteristic of low molecular weights. Although the slope of the $\gamma - \ln c$ curve changes, the coverage does not. This is a result of assumptions i and ii. In a real system, there will be an additional change in slope as the adsorption weakens at low concentrations. One can envisage more realistic situations where the change in surface activity of the different molecular

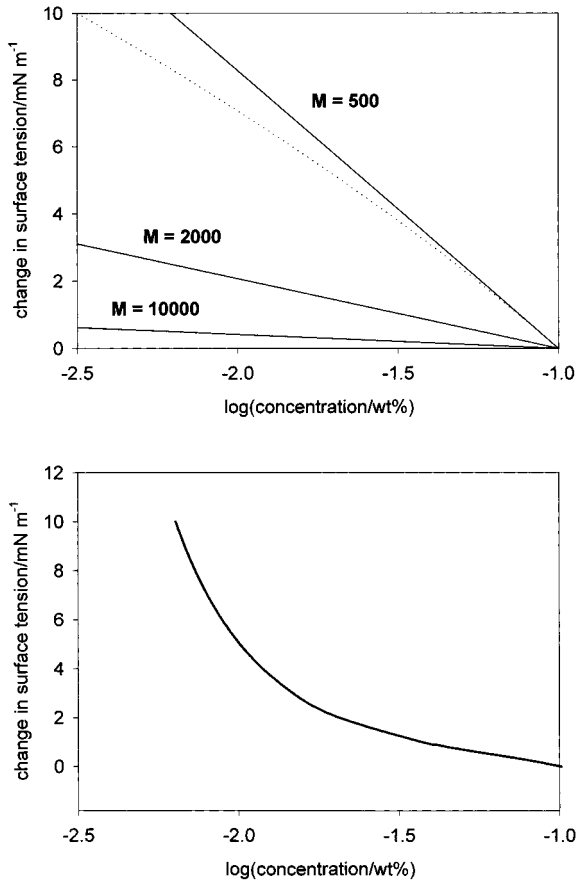

Figure 10. (a) Expected behavior for the variation of surface tension of three different molecular weight samples with concentration, assuming that the *segmental* coverage is independent of both molecular weight and concentration. The dotted line represents a more realistic decrease of surface coverage for the $M = 500$ sample as the concentration is lowered. (b) The variation of surface tension with log(concentration) calculated for a polydisperse polymer sample according to the model described in the text.

weights combined with a particular molecular weight distribution could lead to changes of slope with all components remaining equilibrated with the surface. However, the situation identified here will always occur, i.e., there will be an upwardly curved region associated either with selective depletion or with not all of the species being at equilibrium with the surface. The sharpness of the upturn will evidently be particular to each system. In the previous paper, we have used further assumptions about the distribution and the time scale of the diffusion to calculate a representative $\gamma - \ln c$ plot. This is shown in Figure 10a for a polymer of average M_n of 5000 with a Flory-Schulz distribution and a diffusion cutoff at a molar concentration of around 5×10^{-7} M. The slope of the plot at high concentrations was found in this particular case to approximate to that expected for the average molecular weight, although, at this low molecular weight, a difference of a factor of 2 would not be very noticeable. However, the additional complication of polydispersity in composition and a surface activity that will inevitably vary with composition give the calculation only illustrative value for the case of EPE.

This explanation is different from those presented previously for the low concentration upturn. Further characteristics of the measurements that are consistent with this new explanation are the differences in the measurements by ring and plate and the nonreproducibility of the low concentration measurements on the more monodisperse samples. The more monodisperse the polymer the less the failure of the main species to diffuse to the surface can be compensated by the lower molecular weight species. This may be the explanation for the apparently unexpectedly high low concentration cutoff for the smaller $E_9P_{22}E_9$, which is far too high to be explained by surface depletion effects. The lower molecular weight species will probably have a narrower range of surface activities in its component species.

We have focused on the region around the low concentration break. Around the high concentration break (the CMC), the pattern of adsorption at the air/water interface may be further modified by fractionation of different molecular weight species into the micelles. Linse has applied a mean field treatment to the micellization and shown that the longer components will be preferentially withdrawn from the interfacial region to form micelles.[24] Successive replacement of longer components with shorter ones at the interface above the CMC would then be accompanied by a reduction in the polymer surface excess. Our data gives no information that could disentangle the effects of such fractionation from general changes in the monolayer composition and thickness.

We have given a possible new explanation of the upturn that often seems to occur in the $\gamma - \log c$ plots for water soluble polymeric species. For copolymers, there is the additional complication of polydispersity in composition, which by introducing an even greater variability in surface activity of the different components would reinforce the kind of behavior we have proposed. Whatever the correctness or otherwise of our proposed explanation, the earlier explanation in terms of an abrupt change in the structure of the monolayer is unlikely be correct. The main argument against it is that the Gibbs equation must apply through any structural transition, and given that the low concentration phase would probably be associated with either a decrease in coverage or no significant change, the slope of the curve on the low concentration side of the break should decrease, whereas it increases by a large amount. The neutron reflection results show that there is no abrupt change in coverage that could cause the observed change in slope. Thus, the adsorption isotherm of $E_{23}P_{52}E_{23}$ depicted in Figure 6 shows that in section D the surface excess is increasing steadily with concentration up to about the break but, above the break, the monolayer appears to be complete over the whole range of concentration of region B. A structural rearrangement within the monolayer does occur above 10^{-4} M, almost 2 orders of magnitude higher than the low concentration break.

For $E_{23}P_{52}E_{23}$, neutron reflection gives a value of the area per EO segment at 1.2×10^{-3} M of 6 Å^2, which is much less than the 11−12 Å^2 per EO segment obtained for the $C_{12}E_m$ series of nonionic surfactants at their CMCs,[25] although that of $E_9P_{22}E_9$ at 11.9 Å^2 is about the same. The EO monolayer thicknesses for $C_{12}E_4$, $C_{12}E_5$, $C_{12}E_6$, $C_{12}E_8$, and $C_{12}E_{12}$ at their CMCs are about 21, 22, 25, and 29 ± 2 Å, respectively, where we have scaled the previous data in such a way as to make the model the same for the two types of system. After the removal of roughness, the thicknesses of the EO layers in these molecules were found to scale with the square root of the number of bonds in the EO chain, which would lead to a thickness for E_{23} (69 bonds) of about 40 Å, somewhat less than the 54 Å actually observed and for E_9 25 Å in comparison with the observed value of 49 Å. This could be taken to indicate that closer packing of the EO chain is leading to a change from a Gaussian chain profile to a parabolic profile. However, there are reasons why one should be cautious about such an interpretation. For the $dE_9P_{22}dE_9$, the thickness of the layer is greater than the fully

extended length of the E_9. This should be about 32 Å, taking the fully extended length to be 3.6 Å.[26] The most probable explanation of this is that the PO and EO blocks are extensively mixed and that essentially what is being observed are the dimensions of the molecule as a whole. We discuss this in more detail when we consider the structure of the layer in the subsequent paper.

Acknowledgment. We thank Dow AgroSciences and the Engineering and Physical Science Research Council of the U.K. for financial support.

References and Notes

(1) Schmolka, I. R. *J. Am. Oil Chem. Soc.* **1977**, *54*, 110.
(2) Alexandridis, P. *Coll. Int. Sci.* **1996**, *1*, 490.
(3) Alexandridis, P. *Curr. Opinion Coll. Int. Sci.* **1997**, *2*, 478.
(4) Chu, B.; Zhou, Z. *Surf. Sci. Ser*. **1996**, *60*, 67.
(5) Prasad, K. N.; Luong, T. T.; Florence, A. T.; Paris, J.; Vaution, C.; Seiller, M.; Piusieux, F. *J. Colloid Interface Sci.* **1979**, *69*, 225.
(6) Wanka, G.; Hoffmann, H.; Ulbricht., W. *Macromolecules* **1994**, *27*, 4145.
(7) Alexandridis, P.; Holzwarth, J. F.; Fukuda, S.; Hatton, T. J. *Langmuir* **1994**, *10*, 2604.
(8) Linse, P.; Hatton, T. A. *Langmuir* **1997**, *13*, 4066.
(9) Lu, J. R.; Penfold, J.; Thomas, R. K. *Adv. Colloid Interface Sci.* **2000**, *84*, 143.
(10) Altinok, H.; Yu, G. E.; Nixon, S. K.; Gorry, P. A.; Attwood, D.; Booth, C. *Langmuir* **1997**, *13*, 5837.
(11) Harkins, W. D.; Jordan, H. F. *J. Am. Chem. Soc*. **1930**, *52*, 1751.
(12) Penfold, J.; Richardson, R. M.; Zarbakhsh, A.; Webster, J. R. P.; Bucknall, D. G.; Rennie, A. R.; Jones, R. A. L.; Cosgrove, T.; Thomas, R. K.; Higgins, J. S.; Fletcher, P. D. I.; Dickinson, E.; Roser, S. J.; McLure, I. A.; Hillman, R. A.; Richards, R. W.; Staples, E. J.; Burgess, A. N.; Simister, E. A.; White, J. W. *J. Chem. Soc. Faraday Trans.* **1997**, *93*, 3899.
(13) Alexandridis, P.; Holzwarth, J. F.; Hatton, T. A. *Macromolecules* **1994**, *27*, 2414.
(14) Lopes, J. R.; Loh, W. *Langmuir* **1998**, *14*, 750.
(15) Alexandridis, P.; Athanassiou, V.; Hatton, T. A. *Langmuir* **1995**, *11*, 2442.
(16) Couper, A.; Eley, D. D. *J. Polym. Sci.* **1948**, *3*, 345.
(17) Glass, J. E. *J. Phys. Chem*. **1968**, *72*, 4459.
(18) Malmsten, M.; Linse, P.; Zhang, K. W. *Macromolecules* **1993**, *26*, 2905.
(19) Shinoda, K.; Yamanaka, T.; Kinoshita, K. *J. Phys. Chem. B* **1959**, *63*, 648.
(20) Meguro, K.; Ueno, M.; Esumi, K. *Nonionic Surfactants: Physical Chemistry*; Marcel Dekker: New York, 1987; p 109.
(21) Fleer, G. J.; Cohen Stuart, M. A.; Scheutjens, J. M. H. M.; Cosgrove, T.; Vincent, B. *Polymers at Interfaces*; Chapman & Hall: New York, 1993.
(22) Hines, J. D.; Thomas, R. K.; Garrett, P. R.; Rennie, G. K.; Penfold, J. *J. Phys. Chem. B* **1997**, *101*, 9215.
(23) An, S. W.; Thomas, R. K.; Forder, C.; Billingham, N. C.; Armes, S. P.; Penfold, J. *Langmuir*, in press.
(24) Linse, P. *Macromolecules* **1994**, *27*, 6404.
(25) Lu, J. R.; Su, T. J.; Li, Z. X.; Thomas, R. K.; Staples, E. J.; Tucker, I.; Penfold, J. *J. Phys. Chem. B* **1997**, *101*, 10332.
(26) Takahashi, Y.; Sumita, I.; Tadokoro, H. J. *Polym. Sci*. **1973**, *11*, 2113.